Results in Materials 5 (2020) 100068

Contents lists available at ScienceDirect

Results in Materials

journal homepage: www.journals.elsevier.com/results-in-materials

Advanced thermal stability investigations of the Mn–Al-Ga system

T. Mix *, T.G. Woodcock

Leibniz IFW Dresden, Institute for Metallic Materials, Helmholtzstraße 20, 01069, Dresden, Germany

ARTICLE INFO

Keywords:
Rare earth free permanent magnet
L10
Mn–Al
Mn–Ga
Mn–Al-Ga
Thermal stability

ABSTRACT

A ternary Mn–Al-Ga alloy with the nominal composition $Mn_{55}Al_{38.57}Ga_{6.43}$ was produced by arc melting. After homogenisation, the alloy consisted of the ε and γ_2 phases. Appropriate heat treatments were used to transform each of these into a phase with the $L1_0$ structure. These two $L1_0$ phases had different compositions, lattice parameters and magnetic properties. In order to test the stability of the $L1_0$ phases against decomposition, heat treatments were carried out at 700 °C for durations of up to 14 days. The results showed that the decomposition started with formation of the β-Mn phase and subsequent appearance of the γ_2 phase. The resulting diffusion gradients resulted in composition changes in the $L1_0$ phases and after 7 days, only a single, intermediate composition remained. After 14 days, the decomposition was almost complete. The decomposition of the $L1_0$ phases in the ternary Mn–Al-Ga alloy was significantly slower than in binary Mn–Al alloys.

1. Introduction

The ferromagnetic phases with the $L1_0$ structure at near-equiatomic compositions in the Mn–Al and Mn–Ga binary systems show promising hard magnetic properties [1–4] and are therefore interesting candidates for rare earth free permanent magnets. In both systems, saturation magnetisations of more than 0.75 T were observed and the magnetocrystalline anisotropy constants show values promising for the achievement of coercivities larger than 0.5 T [1,5]. Unfortunately both systems possess disadvantages. Whereas the $L1_0$ phase in Mn–Ga is thermodynamically stable, it is metastable in the Mn–Al system [6,7]. At elevated temperatures in Mn–Al alloys, the metastable phase with the $L1_0$ structure decomposes into the γ_2 and β-Mn equilibrium phases, thus severely limiting the possibility to process the material at elevated temperatures [8]. The common method to tackle this disadvantage is alloying the Mn–Al alloys with carbon [9], but this results in a strong reduction in the Curie temperature [10], which is a significant disadvantage for applications. In the Mn–Ga system, the critical nature of global Ga supplies [11,12] and the high raw materials cost of Ga make the industrial production of bulk materials with approximately 50 at% Ga unthinkable.

One possibility to overcome the problems of the binary systems is the formation of ternary Mn–Al-Ga alloys. Previous work has shown that samples consisting only of $L1_0$ phases can be produced for all alloys of the form $Mn_{55}Al_{45-x}Ga_x$ ($0 \leq x \leq 45$) [5]. In alloys with $5 < x \leq 9$ at.% Ga, the formation of two different $L1_0$ phases was observed. At 1100 °C, the alloys consisted of a mixture of the high temperature ε and γ phases [5]. On cooling at intermediate rate from this temperature the γ phase transformed to γ_2 and the ε phase transformed to $L1_0$ (further referred to as $L1_0(\varepsilon)$), as it does in binary Mn–Al alloys [5]. After annealing the alloy at 500 °C for 2 h, it was observed that the γ_2 phase had also transformed into an $L1_0$ phase (further referred to as $L1_0(\gamma_2)$), as it does in binary Mn–Ga alloys [5]. It was shown that the two $L1_0$ phases are different in their composition, resulting in different lattice parameters and magnetic properties [5]. The average saturation magnetisation showed even superior values compared to the binary end members and was $\mu_0 M_{sat} = 0.848$ T for the $Mn_{55}Al_{39.375}Ga_{5.625}$ alloy [5]. First investigations of the thermal stability in the ternary alloys indicated an improved stability compared to binary Mn–Al: after annealing the ternary alloy at 700 °C for 2 h no decomposition of the $L1_0$ phases was visible in the XRD patterns, whereas for the binary Mn–Al system a strong decomposition in the β-Mn and γ_2 equilibrium phases was observed [5]. BSE images of the annealed ternary alloy nevertheless showed hints of small β-Mn precipitates formed at the grain boundaries, indicating the beginning of the decomposition of at least one of the $L1_0$ phases [5]. The aim of the current work is to better clarify the long-term stability of the $L1_0$ phases at temperatures of 700 °C, which are typical for bulk deformation methods and therefore longer annealing durations of 4 h, 6 h, 24 h, 7 days and 14 days have been carried out and the resulting phase compositions of the alloys have been analysed.

* Corresponding author.
E-mail address: t.mix@ifw-dresden.de (T. Mix).

https://doi.org/10.1016/j.rinma.2020.100068
Received in revised form 22 November 2019; Accepted 16 December 2019
Available online 23 January 2020

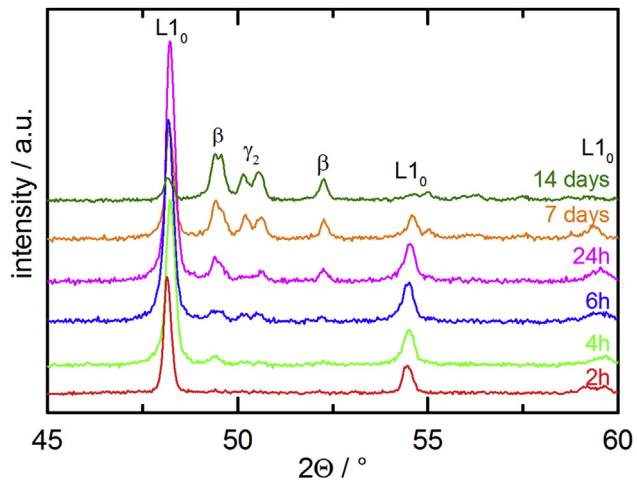

Fig. 1. Partial X-ray diffraction patterns of the $Mn_{55}Al_{38.57}Ga_{6.43}$ alloy at 700 °C for different annealing durations.

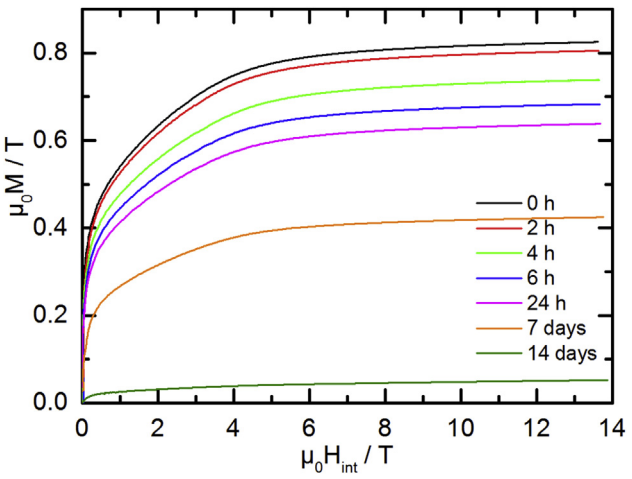

Fig. 3. Magnetisation curves up to 14 T after different annealing times at 700 °C for the $Mn_{55}Al_{38.57}Ga_{6.43}$ alloy.

2. Experimental

The ternary Mn–Al-Ga alloys were produced by arc melting of elemental materials with purity 99.8% for Mn, 99.99% for Al and 99.999% for Ga in the appropriate quantities. The samples were annealed in quartz tubes filled with Ar. For the production of the $L1_0$ phases the annealing was carried out at 1100 °C for 48 h followed by an annealing at 500 °C for 24 h. To investigate the thermal stability of the $L1_0$ phases samples with the composition $Mn_{55}Al_{38.57}Ga_{6.43}$ (with ±1 at.% to the nominal composition) were used and additional heat treatments at 700 °C for 4 h, 6 h, 24 h, 7 days and 14 days carried out. For all heat treatments the furnace was heated to the needed temperature before the samples were inserted. After the annealing the quartz tubes were quenched into water to obtain a fast cooling rate.

The analysis of the crystal structure was done with x-ray diffraction (XRD) using a Bruker diffractometer together with the Rietveld refinement method and the FullProf program [13,14]. Thereby θ - 2θ in the range from 20° to 120° were carried out using Co-K_α radiation ($\lambda(K_{\alpha1}) = 1.78919$ Å; $\lambda(K_{\alpha2}) = 1.79321$ Å; ratio 1:1).

The microstructure of the alloys was observed with a Zeiss Leo Gemini 1530 scanning electron microscope. Additionally the composition of the phases was analysed using an energy dispersive X-ray spectroscopy (EDX) extension from Bruker. The compositions were averaged from at least 5 point measurements per phase. The accuracy of the quantitative EDX measurements can be described as a combination of the experimental inaccuracy together with the statistics of the measurement results and is approximately ±1 atomic percent. The preparation of the samples for microscopy was carried out using standard metallographic methods.

The saturation magnetisation of the samples were measured at an applied field of 14 T in the VSM mode of a Quantum Design PPMS. For the thermomagnetic measurements the same device was used with an applied field of 0.1 T. The samples were non-textured and the demagnetisation factors were calculated according to the sample shape and used to calculate the internal magnetic field H_{int}.

3. Results and discussion

The XRD patterns in the range 45°–60° 2θ are shown in Fig. 1 (The complete XRD patterns can be seen in the supplemental material) clearly indicate a phase transformation during the heat treatment. After 4 h first evidence of β-Mn formation becomes visible. The fraction of β-Mn is increasing with increasing annealing time and additional γ_2 peaks appear after 7 days of annealing, indicating a slow $L1_0$ decomposition over time. Nevertheless after 7 days strong peaks of the $L1_0$ structure are still present. After 14 days at 700 °C the peaks of the β-Mn and γ_2 phases are dominant but clear $L1_0$ reflexes are still visible.

Looking at the microstructure after the individual heat treatments (see Fig. 2) the growth of the β-Mn precipitates (bright regions in the BSE

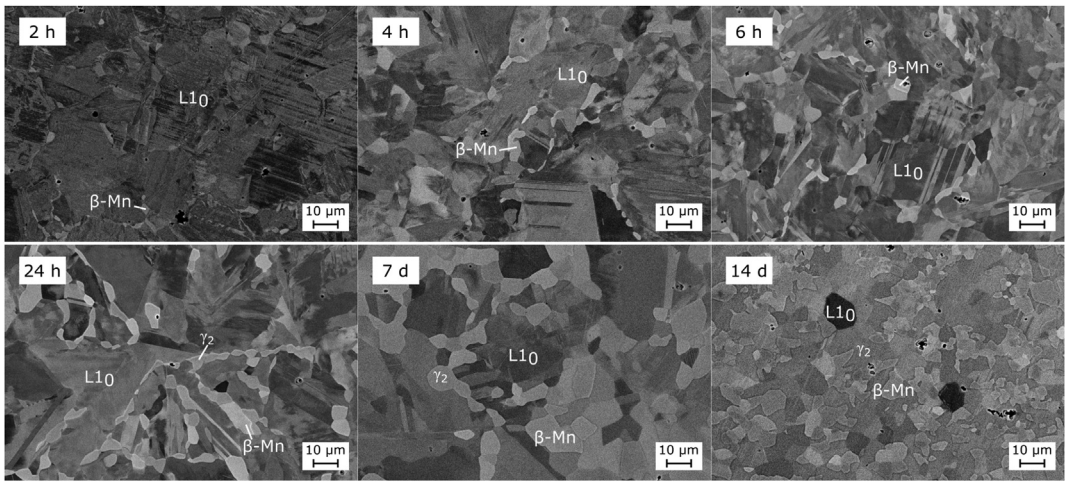

Fig. 2. BSE images of the $Mn_{55}Al_{38.57}Ga_{6.43}$ alloy after the 700 °C annealing for different durations.

in Fig. 2) at the grain boundaries of the $L1_0$ phases can be seen. These precipitates slowly increase in size and volume fraction with increasing annealing durations. After the 7 days three different phases exist. Two of the phases appear bright in the BSE images which can be identified as β-Mn and γ_2 with the help of EDX analysis. The dark regions in the BSE images correspond to the $L1_0$ phase. The composition of the β-Mn phase was found to be $Mn_{59.1}Al_{37.6}Ga_{3.3}$ (see Table 1). The high amount of manganese is consistent to the β-Mn region in the binary phase diagrams leading to the identification as the β-Mn phase. For the second bright phase a composition of $Mn_{49.1}Al_{42.8}Ga_{8.1}$ was determined. With the reduced amount of Mn in this region an identification as γ_2 is suggested. The remaining $L1_0$ phase shows a composition of $Mn_{53.1}Al_{40.2}Ga_{6.7}$ and thus the composition of the phase is located between the initial compositions of the $L1_0(\varepsilon)$ and $L1_0(\gamma_2)$ phases. As the Mn content is strongly enriched in the β-Mn phase, diffusion of Mn would be necessary for the formation of the β-Mn phase and therefore for the decomposition of the $L1_0$ phase. Additionally, the Ga content of the β-Mn phase is noticeably lower than that of the other phases. This may indicate a lower solubility of Ga in β-Mn and implies that, in addition to Mn enrichment through diffusion, Ga must also diffuse away from a region in order to form β-Mn. The decomposition into β-Mn and later on into γ_2 is therefore accompanied with a strong diffusion leading into a change of the initial $L1_0$ compositions. This assumption is strengthened by the results of the 14 days annealing at 700 °C. After this duration, a large fraction of the sample was transformed into β-Mn and γ_2. Only some $L1_0$ grains can be found in the BSE images. A clear distinction between the two $L1_0$ phases is no longer possible. The mean composition of the $L1_0$ phase was found to be $Mn_{52.3}Al_{40.0}Ga_{7.7}$, which lies between that of the $L1_0(\varepsilon)$ and $L1_0(\gamma_2)$ initial $L1_0$ phases.

The individual compositions of the different phases after each annealing is collected in Table 1. There one can see that composition of the β-Mn and γ_2 phase are relative constant after each annealing step whereas the composition of the $L1_0$ phases changes slightly. Especially after 7 and 14 days the diffusion driven change of the $L1_0$ phase is visible.

Magnetic measurements of the alloys after the heat treatments can be used to give an idea of the remaining volume fraction of the $L1_0$ phases (see Fig. 3). Up to 24 h more than 77% of the magnetic $L1_0$ phase was retained. With increasing annealing to 7 days at 700 °C the fact that still about half of the sample consists of $L1_0$ is remarkable. This stands in good accordance with microstructural investigation. Compared to the binary Mn–Al system this is a huge improvement. Even for alloys with carbon addition it was reported that only one-third of the $L1_0$ phase was not decomposed after 7 days of annealing at 700 °C [15]. In the case of the ternary Mn–Al-Ga alloy after the same time still more than 50% of the sample remains in the $L1_0$ phase. After 14 days according to the magnetisation 6% of the $L1_0$ remained.

Additionally to the hysteresis curves thermomagnetic measurements were carried out to investigate the change of the Curie temperature with the different annealing durations. For the two different $L1_0$ phases these measurements clearly showed two different Curie temperatures as they are strongly depending on the compositions. This behaviour can also be seen up to 24 h of annealing at 700 °C as shown in Fig. 4. For longer

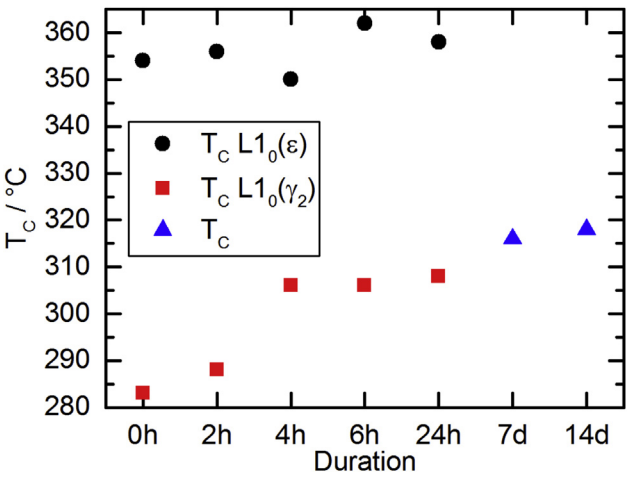

Fig. 4. Curie temperature changes after different annealing durations of the $Mn_{55}Al_{38.57}Ga_{6.43}$ alloy. Up to 24 h of annealing for the two different $L1_0$ phases with different compositions 2 Ci temperatures could be found. For 7 and 14 days only 1 Ci temperature remained.

annealing times the typical two step behaviour of the thermomagnetic measurement is not visible anymore. Resulting in only one remaining Curie temperature of $T_C = 318$ °C for the $L1_0$ phase with intermediate composition. It is interesting to note that the T_C of the single $L1_0$ phase is closer to that of the $L1_0(\gamma_2)$ phase although the composition of the single $L1_0$ phase is closer to that of $L1_0(\varepsilon)$.

4. Conclusion

Extending the heat treatments of the ternary Mn–Al-Ga alloys up to two weeks at 700 °C allowed a better understanding of the thermal stability of the $L1_0$ phase. It could be shown that the two different $L1_0$ phases $L1_0(\gamma_2)$ and $L1_0(\varepsilon)$ possess an increased thermal stability compared to binary Mn–Al. The beginning of the decomposition process could be observed in the XRD after 4 h and in magnetic measurements after 2 h of annealing at 700 °C. The decomposition of the $L1_0$ phase seems to be diffusion driven and starts with the formation of β-Mn. The first hints of the second equilibrium phase (γ_2) were observed after 6 h of annealing. More than 77 vol% of the $L1_0$ phases remained after 24 h of annealing at 700 °C. This is a large improvement compared to binary Mn–Al. The composition of the $L1_0$ phases changes with increased annealing time and results in one final intermediate composition. After 7 days over 50% of the sample remained in this intermediate $L1_0$ phase. An additional 7 days of annealing, resulting in an overall duration of 14 days, led to further decomposition with 6 vol% $L1_0$ phase remaining at the end. Thermomagnetic measurements confirmed the change of the composition from two distinct $L1_0$ phases to one single composition with increasing annealing duration: the Curie temperature of the final $L1_0$ phase was found to be $T_C = 318$ °C. Overall, the higher thermal stability of the ternary alloys compared to binary Mn–Al is promising; however,

Table 1
Compositions of the different phases inside the $Mn_{55}Al_{38.57}Ga_{6.43}$ alloy obtained from at least 20 point measurements for the $L1_0$ phases and more than 5 points for β-Mn and γ_2 resulting in an accuracy of ±1 at.% after different annealing times at 700 °C measured with EDX method.

Duration	$L1_0(\varepsilon)$ (at.%)			$L1_0(\gamma_2)$ (at.%)			$L1_0$ (at.%)			β-Mn (at.%)			γ_2 (at.%)		
	Mn	Al	Ga	Mn	Al	Ga	Mn	Al	Ga	Mn	Al	Ga	Mn	Al	Ga
0 h	54.9	39.0	6.1	51.6	41.3	7.0									
2 h	54.6	39.1	6.3	51.4	41.2	7.3									
4 h	54.1	39.4	6.5	50.9	41.8	7.3									
6 h	54.3	39.4	6.3	51.3	41.6	7.1				58.7	37.4	3.9	48.5	43.7	7.8
24 h	53.7	39.6	6.7	51.8	40.9	7.3				58.5	37.6	3.9	48.7	43.2	8.1
7 d							53.1	40.2	6.7	59.1	37.6	3.3	49.1	42.8	8.1
14 d							52.3	40.0	7.7	58.6	37.8	3.6	48.8	42.7	8.5

from the results presented here, it is not possible to assess whether one of the two original $L1_0$ phases could be thermodynamically stable at 700 °C. Producing samples consisting of only one of these phases is therefore highly important in order to be able to characterise the thermal stability in the absence of the diffusion gradients which led to the decomposition in the current work.

Acknowledgements

This work was funded by the Deutsche Forschungsgemeinschaft (DFG, German Research Foundation) – Project number: 380033763. The publication of this article was funded by the Open Access Fund of the Leibniz Association.

Appendix A. Supplementary data

Supplementary data to this article can be found online at https://doi.org/10.1016/j.rinma.2020.100068.

References

[1] J.M.D. Coey, Permanent magnets: plugging the gap, Scripta Mater. 67 (2012) 524–529.
[2] R. Skomski, J.M.D. Coey, Magnetic anisotropy — how much is enough for a permanent magnet? Scripta Mater. 112 (2016) 3–8.
[3] H.G. Meissner, K. Schubert, T.A. Anantharaman, The constitution and structure of manganese-gallium alloys, Proc. Indian Acad. Sci. Sect. A 61 (1965) 340.
[4] T. Mix, K.-H. Müller, L. Schultz, T.G. Woodcock, Formation and magnetic properties of the $L1_0$ phase in bulk, powder and hot compacted Mn–Ga alloys, J. Magn. Magn Mater. 391 (2015) 89–95.
[5] T. Mix, F. Bittner, K.-H. Müller, L. Schultz, T.G. Woodcock, Alloying with a few atomic percent of Ga makes MnAl thermodynamically stable, Acta Mater. 128 (2017) 160–165.
[6] T.B. Massalski, U.R. Kattner, Binary Alloy Phase Diagrams, ASM International, Ohio, 1990.
[7] H. Kono, On the ferromagnetic phase in manganese-aluminum system, J. Phys. Soc. Japan. 13 (12) (1958) 1444–1451.
[8] W. Koester, E. Wachtel, Aufbau und magnetische Eigenschaften der Aluminium-Mangan-Legierungen mit mehr als 25 At.% Mn, Zeitschrift Für Met. 51 (1960) 271–280.
[9] T. Ohtani, N. Kato, S. Kojima, K. Kojima, Y. Sakamoto, I. Konno, M. Tsukahara, T. Kubo, Magnetic properties of Mn-Al-C permanent magnet alloys, IEEE Trans. Magn. (1977) 1328–1330.
[10] L. Pareti, F. Bolzoni, F. Leccabue, A.E. Ermakov, Magnetic anisotropy of MnAl and MnAlC permanent magnet materials, J. Appl. Phys. 59 (1986) 3824.
[11] European Commission, Report on Critical Raw Materials for the EU: Critical Raw Materials Profiles, 2014.
[12] European Commission, Study on the review of the list of critical raw materials, Eur. Comissmion. (2017) 93.
[13] J. Rodríguez-Carvajal, FullProf for Magnetic Structure Determination and Refinement, (n.d.).
[14] J. Rodriguez-Carvajal, T. Roisnel, FullProf.98 and WinPLOTR: New Windows 95/NT Applications for Diffraction Commission for Powder Diffraction, International Union for Crystallography, 1998.
[15] W. Dreizler, A. Menth, Transformation kinetics of the ferromagnetic alloy Mn-Al-C, IEEE Trans. Magn. 16 (1980) 534–536.